Contribution from the Departament de Química Inorgànica (UIBCM), Facultat de Ciències Químiques, Universitat de València, C/ Dr. Moliner 50, 46100 Burjassot, València, Spain, and Institut de Ciència de Materials de Barcelona (CSIC), 08193 Bellaterra, Barcelona, Spain

Structural and Magnetic Characterization of $CaCu(HCOO)_4$ and $Ca_2Cu(HCOO)_6$: Two New One-Dimensional Ferromagnetic Bis(μ-oxo-ligand)-Bridged Chains

Maria J. Sanchis,[†] Pedro Gómez-Romero,[‡] José-Vicente Folgado,[†] Fernando Sapiña,[†] Rafael Ibáñez,[†] Aurelio Beltrán,[†] Juana García,[†] and Daniel Beltrán*[,†]

Received November 14, 1991

The structures of two novel calcium and copper formates, $CaCu(HCOO)_4$ (**1**) and $Ca_2Cu(HCOO)_6$ (**2**), have been determined by X-ray methods. Both formates crystallize in monoclinic systems, space groups $P2/c$ (**1**) and $C2/c$ (**2**), with $Z = 2$ (**1**) and $Z = 4$ (**2**). The dimensions of the cells are $a = 7.300$ (2) Å, $b = 8.493$ (2) Å, $c = 6.449$ (2) Å, and $\beta = 97.57$ (1)° for (**1**) and $a = 22.296$ (2) Å, $b = 8.803$ (2) Å, $c = 6.377$ (4) Å, and $\beta = 101.00$ (5)° for (**2**). Least-squares refinements of 595 (**1**) and 934 (**2**) reflections ($I > 3\sigma$) and 71 (**1**) and 106 (**2**) parameters gave a final R of 0.027 for (**1**) and 0.024 for (**2**). In both cases the structure involves chains of bis(μ-formate)-bridged copper(II) ions connected to calcium chains through formate bidentate groups. The metallic chains run practically parallel to the c axis and alternate along the a axis giving ...–Ca–Cu–Ca–... (**1**) and ...–Ca–Ca–Cu–Ca–Ca–... (**2**) sequences. Magnetic susceptibility measurements show a behavior typical of infinite arrays of spins ferromagnetically coupled. Single-crystal electron paramagnetic resonance spectroscopic data are characteristic of one-dimensional magnetic materials with line widths following a $[(3\cos^2\theta) - 1]^{4/3}$ dependence.

Introduction

In a recent publication, Müller-Buschbaum refers to the world-wide awakening of interest in copper-containing oxide compounds as a result of the euphoria surrounding the high-temperature oxide superconductors.[1] In that work, he points out that attempts to prepare the superconductor related $CaCuO_2$ compound have invariably failed. The fact is that we have just reported a low-temperature clean synthesis both of this oxide, $CaCuO_2$, and the related Ca_2CuO_3 starting from two novel bimetallic formates as chemical precursors.[2] Additionally, we have previously discussed in detail the potential advantages of lower mixed carboxylates when looking for basic-metal cuprate precursors.[3]

In the present work we describe the crystal structures, the magnetic properties, and the EPR spectra of these two new calcium and copper formates, $CaCu(HCOO)_4$ and $Ca_2Cu(HCOO)_6$. As shown below, besides their aforementioned interest as oxide precursors, the presence in both compounds of copper linear chains involving bis(μ-oxo-ligand) bridges contitutes a rather unusual feature. Actually, as far as we know, such a copper bis(μ-carboxylate)-bridged structural unit only has been found in a few dimeric compounds.[4,5] Its presence has been suggested, however, in one of the several modifications of anhydrous copper(II) formate.[6,7] Notwithstanding, there are no crystal data on this variety, obtained by dehydration of copper(II) formate tetrahydrate, and the structural proposal[6] was formulated considering the topotactic character of the dehydration process. The involvement of these peculiar copper chains in the title compounds led us to study their magnetic properties. As might be expected, both materials behave as one-dimensional ferromagnets.

Experimental Section

Preparation of the Complexes $CaCu(HCOO)_4$ (1) and $Ca_2Cu(HCOO)_6$ (2). Both formate complexes are easily prepared by slowly adding the required stoichiometric amount of $CaCO_3$ to a solution of $CuCO_3 \cdot Cu(OH)_2 \cdot 2H_2O$ (13.7 mmol) in the minimum amount needed (ca. 50 mL) of a 20% formic acid solution. Polycrystalline powders are readily obtained in good yield by evaporation at 45–50 °C. The growth of prismatic blue (**1**) and blue-green (**2**) single crystals suitable for X-ray structure determination requires slow evaporation (several days) at room temperature. C and H contents in the solids were determined by elemental analysis. Copper and calcium were determined by atomic absorption using a Perkin-Elmer 300 AA spectrophotometer. Anal. Found (calcd) for **1**: Ca, 13.8 (14.1); Cu, 22.1 (22.4); C, 17.0 (16.8); H, 1.30 (1.42). Anal. Found (calcd) for **2**: Ca, 19.0 (19.4); Cu, 15.2 (15.3); C, 17.5 (17.4); H, 1.45 (1.46).

Table I. Crystallographic Data for $CaCu(HCOO)_4$ and $Ca_2Cu(HCOO)_6$

compound	$CaCu(HCOO)_4$	$Ca_2Cu(HCOO)_6$
empirical formula	$CaCuH_4C_4O_8$	$Ca_2CuH_6C_6O_{12}$
FW	283.69	413.80
cryst syst	monoclinic	monoclinic
space group	$P2/c$	$C2/c$
a, Å	7.300 (2)	22.296 (8)
b, Å	8.493 (2)	8.803 (2)
c, Å	6.449 (2)	6.377 (4)
β, deg	97.57 (1)	101.00 (5)
V, Å^3	396.4	1228.6
Z	2	4
T, °C	22	22
λ, Å	0.7093	0.7093
ρ_{calcd}, g/mL	2.377	2.237
linear abs coeff, cm^{-1}	33.54	26.0
$R(F_o)^a$	0.027	0.024
$R_w(F_o)^b$	0.030	0.026

$^a R = \sum||F_o| - |F_c||/\sum|F_o|$. $^b R_w = [\sum w||F_o| - |F_c||^2/\sum w|F_o|^2]^{1/2}$.

Structure Determination of $CaCu(HCOO)_4$ (1) and $Ca_2Cu(HCOO)_6$ (2). X-ray data were recorded using a CAD-4 Enraf Nonius diffractometer. The intensities of three standard reflections, measured every 100 reflections, were monitored throughout the data collection. In both cases, no significant variation was detected. Lattice parameters were obtained by the centering of 25 strong reflections at high 2θ angles. Other important features of data collection are summarized in Table I.

Precession photos of a crystal of **1** showed symmetry and systematic absences consistent with space groups $P2/c$ and Pc, whereas in the case of **2** the systematic absences (hkl, $h + k = 2n$; $h0l$, $l = 2n$; ($h = 2n$)) were consistent with space groups Cc and $C2/c$. The structures were solved with MULTAN-84[8] and developed with SHELX-76[9] using successive full-

[†] Departament de Química Inorgànica (UIBCM), Facultat de Ciènces Químiques, Universitat de València, c/ Dr. Moliner 50, 46100 Burjassot, València, Spain.

[‡] Institut de Ciencia de Materials de Barcelona (CSIC), 08193, Bellaterra, Barcelona, Spain.

(1) Müller-Buschbaum, H. *Angew. Chem., Int. Ed. Engl.* **1991**, *30*, 723.
(2) Sanchis, M. J.; Sapiña, F.; Ibáñez, R.; Beltrán, A.; Beltrán, D. *Mater. Lett.* **1992**, *12*, 409–414.
(3) Beltrán-Porter, D.; González, A.; Sanchis, M. J.; Beltrán-Porter, A.; Ibáñez, R.; Sapiña, F. In *Ceramic Transactions (Superconductivity and Ceramic Superconductors II)*; American Ceramic Society: Westerville, OH, 1991; Vol. 18, p 191.
(4) Costes, J. P.; Dahan, F.; Laurent, J. P. *Inorg. Chem.* **1985**, *24*, 1018.
(5) Kato, M.; Muto, Y. *Coord. Chem. Rev.* **1988**, *92*, 45.
(6) Günter, J. R. *J. Solid State Chem.* **1980**, *35*, 43.
(7) Towle, D. K.; Hoffmann, S. K.; Hatfield, W. E.; Singh, P.; Chaudhuri, P. *Inorg. Chem.* **1988**, *27*, 394.
(8) Main, P.; Germain, G.; Woolfson, M. M. *MULTAN 11/84, System of Computer Programs for the Automatic Solution of Crystal Structures from X-ray Diffraction Data*; Universities of York and Louvain: York, England, and Louvain, Belgium, 1984.
(9) Sheldrick, G. M. *Program for Crystal Structure Determination*; University of Cambridge: Cambridge, 1976.

0020-1669/92/1331-2915$03.00/0

Table II. Positional and Equivalent Isotropic Thermal Parameters for $CaCu(HCOO)_4$ (**1**) and $Ca_2Cu(HCOO)_6$ (**2**)[a]

atom	x/a	y/b	z/c	B_{eq}, Å^2
		1		
Cu	5000 (0)	4023 (1)	7500 (0)	1.71
Ca	0000 (0)	1359 (1)	7500 (0)	1.45
O(1)	3556 (3)	4365 (3)	0821 (4)	1.95
O(2)	1908 (3)	0423 (3)	4668 (4)	2.37
O(3)	3168 (3)	2374 (3)	6562 (3)	1.90
O(4)	0856 (3)	3153 (3)	0107 (4)	2.39
C(1)	1952 (5)	3988 (4)	1202 (5)	1.85
C(2)	3126 (5)	1437 (4)	5044 (6)	2.01
H(1)	1785 (53)	4290 (44)	2337 (63)	2.37
H(2)	4029 (54)	1436 (45)	4153 (58)	2.37
		2		
Cu	0000 (0)	−0955 (0)	2500 (0)	1.65
Ca	1596 (0)	−3664 (1)	4387 (1)	1.47
O(11)	0475 (1)	0618 (2)	1396 (3)	1.93
O(12)	1362 (1)	1820 (2)	1690 (3)	2.69
O(21)	0602 (1)	−2539 (2)	2178 (3)	2.01
O(22)	0946 (1)	−5487 (2)	5692 (3)	2.48
O(31)	2096 (1)	−1853 (3)	2821 (4)	3.92
O(32)	2146 (1)	−4573 (2)	7771 (3)	2.09
C(1)	1018 (1)	0939 (3)	2302 (4)	2.02
C(2)	0570 (1)	−6504 (3)	5664 (4)	2.09
C(3)	2647 (1)	−3899 (3)	8347 (5)	2.04
H(1)	1156 (14)	0518 (34)	3365 (59)	3.14
H(2)	0223 (13)	−6585 (37)	4452 (49)	3.14
H(3)	2842 (14)	−3949 (35)	9760 (52)	3.14

[a] Standard deviations in the least significant digit are in parentheses. Anisotropically refined atoms are given in the form of the isotropic equivalent displacement parameter defined as: $(4/3)[a^2B(1,1) + b^2B(2,2) + c^2B(3,3) + ab(\cos\gamma)B(1,2) + ac(\cos\beta)B(1,3) + bc(\cos\alpha)B(2,3)]$.

matrix least-squares refinements and difference Fourier syntheses.

The structure of **1** was successfully refined in the centrosymmetric space group $P2/c$, being the final reliability factors $R = 0.027$ and $R_w = 0.030$. All non-hydrogen atoms were refined anisotropically. The hydrogen atoms from formate groups were found using difference Fourier maps and were assigned fixed thermal parameters. A final difference Fourier synthesis was essentially featureless (max. 0.58 e/Å^3 close to Cu, then smooth at ca. 0.27 e/Å^3). The final data parameter ratio was 595/71. Final atomic parameters are listed in Table II, and selected bond distances and angles are given in Table III.

In the case of **2**, when space group Cc was tried, large correlation coefficients between the corresponding parameters resulted. Space group $C2/c$ was confirmed by the good final refinement of the structure. All non-hydrogen atoms were refined anisotropically. Hydrogen atoms were located through difference Fourier and were assigned a common isotropic thermal parameter. The final reliability factors were $R = 0.024$ and $R_w = 0.026$. A final difference Fourier synthesis was essentially featureless (max. 0.55 e/Å^3, close to Cu). The final data/parameter ratio was 934/106. Final atomic parameters are listed in Table II and selected bond distances and angles are given in Table III.

Tables of calculated and observed Structure Factor Amplitudes are available as supplementary material. The geometrical calculations were performed with XANADU.[10]

Physical Measurements. Polycrystalline powder and single-crystal EPR spectra of **1** and **2** were recorded at room temperature on a Varian E15 spectrometer working at 35 GHz and using DPPH ($g = 2.0037$) as internal reference. Prismatic single crystals of **1** and **2** were oriented on the precession camera used for the preliminary studies. The crystals of $CaCu(HCOO)_4$ showed well-developed faces ($\pm1, 0, 0$), ($0, \pm1, 0$), and ($0, \pm1, \pm1$), whereas the more developed ones in the crystals of $Ca_2Cu(HCOO)_6$ were ($\pm1, 0, 0$) and ($\pm1, \pm1, 0$).

ac susceptibility measurements were performed on powdered samples in the temperature range 4.2–60 K using a Lake Shore Cryotonics, Inc., Model 7000 A.C. The frequency was 666.6 Hz and the exciting field amplitude was 10 Oe. Both components of the ac susceptibility, in-phase χ' and out-of-phase χ'', were recorded. Within experimental error, χ'' remains zero for both compounds. Experimental susceptibilities were corrected for both the diamagnetic contributions and the TIP of the Cu(II) ion, estimated to be 60×10^{-6} emu mol^{-1} per Cu(II) ion.[11]

(10) Roberst, P.; Sheldrick, G. M. *XANADU, Program for Crystallographic Calculations*; University of Cambridge: Cambridge, 1975.

Table III. Selected Bond Distances (Å) and Angles (deg) for $CaCu(HCOO)_4$ (**1**) and $Ca_2Cu(HCOO)_6$ (**2**)[a]

Distances

1		2	
Cu–O(1)	1.964 (2) (×2)	Cu–O(11)	1.954 (2) (×2)
Cu–O(1)	2.525 (2) (×2)	Cu–O(11)	2.525 (2) (×2)
Cu–O(3)	1.982 (2) (×2)	Cu–O(21)	1.973 (2) (×2)
Ca–O(2)	2.382 (2) (×2)	Ca–O(12)	2.314 (2)
Ca–O(2)	2.565 (2) (×2)	Ca–O(22)	2.586 (2)
Ca–O(3)	2.610 (2) (×2)	Ca–O(22)	2.415 (2)
Ca–O(4)	2.292 (2) (×2)	Ca–O(22)	2.628 (2)
		Ca–O(31)	2.282 (2)
		Ca–O(32)	2.406 (2)
		Ca–O(32)	2.294 (2)
Cu–Cu- (intrachains)	3.625 (2)	Cu–Cu- (intrachains)	3.605 (2)
Cu–Cu- (interchains)	7.295 (2)	Cu–Cu- (interchains)	11.326 (2)

Angles

1		2	
O(1)–Cu–O(1)	91.88 (1)	O(11)–Cu–O(11)	89.81 (1)
O(1)–Cu–O(1)	97.88 (1) (×2)	O(11)–Cu–O(11)	73.54 (1) (×2)
O(1)–Cu–O(1)	72.79 (1) (×2)	O(11)–Cu–O(11)	96.71 (1) (×2)
O(1)–Cu–O(1)	166.69 (1)	O(11)–Cu–O(11)	166.49 (1)
O(1)–Cu–O(3)	162.68 (1) (×2)	O(11)–Cu–O(21)	92.12 (1) (×2)
O(1)–Cu–O(3)	91.83 (1) (×2)	O(11)–Cu–O(21)	164.68 (1) (×2)
O(1)–Cu–O(3)	99.37 (1) (×2)	O(11)–Cu–O(21)	98.42 (1) (×2)
O(1)–Cu–O(3)	89.95 (1) (×2)	O(11)–Cu–O(21)	91.14 (1) (×2)
O(3)–Cu–O(3)	89.63 (1)	O(21)–Cu–O(21)	90.03 (1)
Ca–O(3)–Cu	138.3 (1)	Ca–O(21)–Cu	138.0 (1)
Cu–O(1)–Cu	107.15 (1)	Cu–O(11)–Cu	106.46 (1)

[a] Standard deviations in the least significant digit are in parentheses.

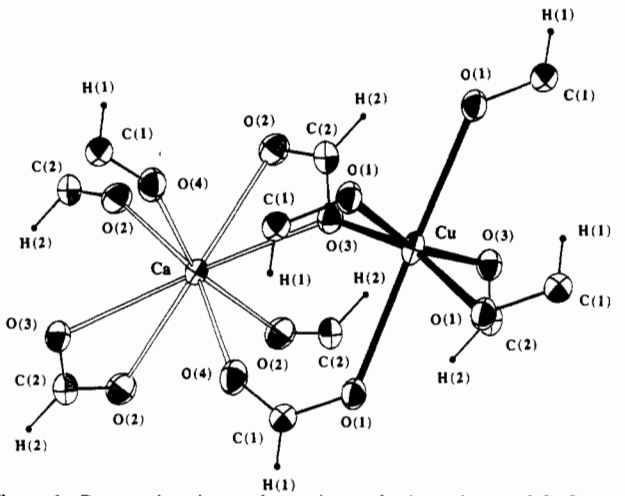

Figure 1. Perspective view and atomic numbering scheme of $CaCu(HCOO)_4$. The thermal ellipsoids are drawn at the 50% probability level for the non-hydrogen atoms and with an arbitrary fixed radius for the hydrogen atoms.

Results and Discussion

Crystal Structures. In both cases the structure involves a tridimensional array of Cu(II) and Ca(II) ions bridged through formate bidentate groups. The formate bridge networks result in chains of edge sharing $[CuO_6]$ pseudo-octahedra which are effectively isolated from each other by chains of Ca(II) ions. According to Willett's notation,[12] the stacking pattern of the $[CuO_4]$ units in the chains is, in both cases, of type II. Both copper and calcium chains run practically parallel to the c axis and alternate along the a axis in such a way that sequences ...–Ca–Cu–Ca–Cu–Ca–... (**1**) and ...–Ca–Ca–Cu–Ca–Ca–... (**2**) result.

The coordination polyhedron around copper(II) can be described, in both compounds, as an axially elongated $[CuO_6]$ oc-

(11) Earnshaw, A. *Introduction to Magnetochemistry*; Academic Press: London and New York, 1968.

(12) Manfredini, T.; Pellacani, G. C.; Bonamartini-Corradi, A.; Battaglia, L. P.; Guarini, G. G. T.; Gelsonimi Giusti, J.; Pon, G.; Willett, D. *Inorg. Chem.* **1990**, *29*, 2221.

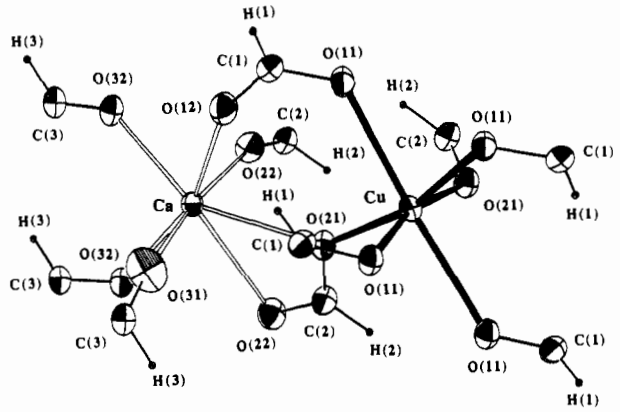

Figure 2. Perspective view and atomic numbering scheme of $Ca_2Cu(HCOO)_6$. The thermal ellipsoids are drawn at the 50% probability level for the non-hydrogen atoms and with an arbitrary fixed radius for the hydrogen atoms.

tahedron in which one axial and one equatorial oxygen atom bridge the metal (in a monoatomic type conformation) with neighboring copper atoms in each chain (Figures 1 and 2). All the Cu–O distances (1.96–2.53 Å in **1**, 1.95–2.53 Å in **2**) are similar to those found in related complexes.[13-15] The equatorial positions are occupied by four oxygen atoms of different formate groups. The four oxygen atoms are not strictly coplanar, with the departures from the mean planes of ±0.2958 and ±0.2617 for **1** and **2**, respectively. Two of the equatorial oxygen atoms belong to type a-4_3-a carboxylate groups (O3 and O3* in **1** and O21 and O21* in **2**) and the other two (O1 and O1′ in **1** and O11 and O11′ in **2**) come from the s-3-sa carboxylates.[16,17] The oxygen atoms in the apical sites (O1* and O1*′ in **1** and O11* and O11*′ in **2**) belong also to the latter s-3-sa carboxylate groups which then act as bidentate ligands toward the copper(II) ion. Given that the $Cu-O_{axial}$ distances ($d_{Cu-O_{ax}}$ = 2.525 (2) Å in both compounds) are significantly longer than the Cu–O equatorial ones ($d_{Cu-O_{eq}}$ = 1.9730 (2) Å in **1**, $d_{Cu-O_{eq}}$ = 1.9635 (2) Å in **2**), the coordination of copper may be viewed as 4 + 2, which is usually found for Jahn–Teller active six-coordinate copper(II) complexes.[18] The tetragonality, T (a phenomenological parametrization of the distortion defined by Hathaway as the mean in-plane Cu–O bond length divided by the mean out-of-plane Cu–O bond length)[18a,d] is 0.80 and 0.78 for **1** and **2**, respectively. These values are smaller (i.e., the distortion is more pronounced) than most of those found for six-coordinated copper(II) complexes;[19] for example, in the chemically related barium copper formate, $Ba_2Cu(HCOO)_6{\cdot}4H_2O$, T = 0.915.[20]

The coordination environment around calcium(II) differs from **1** (Figure 1) to **2** (Figure 2). In the case of **1**, the Ca(II) coordination sphere consists of eight oxygen atoms arranged in the corners of a distorted (C_2) dodecahedron. Four of them [O2, O2′, O3, O3*] belong to two chelating a-4_3-a formate groups, and the other four [O2*, O2*′, O4, O4*] belong to four monodentate ones which behave as a-4_3-a [O2*, O2*′] or s-3-sa [O4, O4*]. On the other hand, calcium is seven-coordinated in **2**. The polyhedron

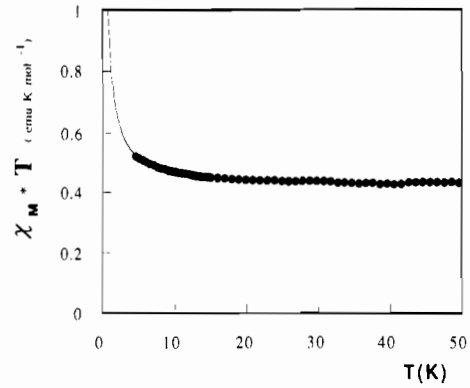

Figure 3. Temperature dependence of the magnetic susceptibility for $CaCu(HCOO)_4$. The solid line represents the calculated values with the best fit parameters (see text).

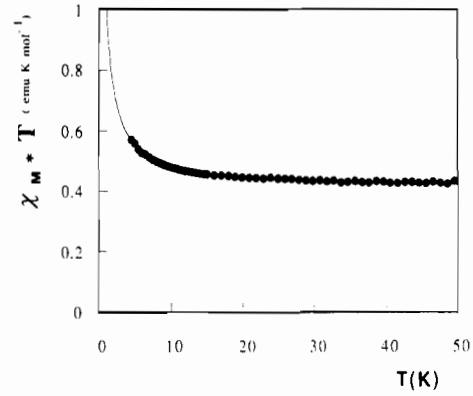

Figure 4. Temperature dependence of the magnetic susceptibility for $Ca_2Cu(HCOO)_6$. The solid line represents the calculated values with the best fit parameters (see text).

around Ca(II) is best described as a distorted capped trigonal prism (C_s). Among these seven oxygen atoms, four [O21, O22, O31, O32] belong to two chelating (a-4_3-a [O21, O22] and 4 [O31, O32]) carboxylates and the other three belong to three different (a-4_3-a, 0.22; s-3-sa, O12; 4, O32*) ligands.

The intrachain copper–copper distance is close to 3.6 Å in both compounds, while the shortest distance between copper atoms from different chains goes from 7.3 Å for **1** to 11.5 Å for **2**.

Magnetic Properties. The magnetic behavior of **1** and **2** is illustrated in Figures 3 and 4, respectively, by means of plots of $\chi_M T$ vs T in the temperature range 4.2–50 K. In both cases, the product $\chi_M T$ is nearly temperature-independent for $T > 20$ K. The observed values, ca. 0.43 emu K mol^{-1}, are close to those expected for one uncoupled $^1/_2$ spin. At lower temperatures the increase of the $\chi_M T$ values (somewhat more pronounced in the case of **2**) indicates the presence of ferromagnetic coupling between Cu(II) ions. Taking into account the crystal structures of these two compounds, the magnetic behavior may be described by the series expansion for the Heisenberg model ($H = -2J\sum_i S_i S_{i+1}$) for ferromagnetically coupled $S = {}^1/_2$ ions that was derived by Baker et al.[21] The expansion is given by eq 1, where $x = 2|J|/kT$.

$$\chi = \frac{Ng^2\beta^2}{4kT}\left[\frac{1 + Ax + Bx^2 + Cx^3 + Dx^4 + Ex^5}{1 + A'x + B'x^2 + C'x^3 + D'x^4}\right]^{2/3} \quad (1)$$

$$A = 5.797\,991\,6 \qquad A' = 2.797\,991\,6$$
$$B = 16.902\,653 \qquad B' = 7.008\,678\,0$$
$$C = 29.376\,885 \qquad C' = 8.653\,864\,4$$
$$D = 29.832\,959 \qquad D' = 4.574\,311\,4$$
$$E = 14.036\,918$$

(13) Barclay, G. A.; Kennard, C. H. L. *J. Chem. Soc.* **1961**, 3289.
(14) Baggio, R. F.; Perazzo, P. K.; Polla, G. *Acta Crystallogr.* **1985**, *C41*, 194.
(15) Klop, E. A.; Duisenberg, A. J. M.; Spek, A. L. *Acta Crystallogr.* **1983**, *C39*, 1342.
(16) Porai-Koshits, M. A.; Pozhidaev, A. I.; Polynova, T. N. *Zh. Strukt. Khim.* **1974**, *15*, 1117.
(17) Porai-Koshits, M. A. *Zh. Strukt. Khim.* **1980**, *21*, 146.
(18) (a) Hathaway, B. J.; Billing, D. E. *Coord. Chem. Rev.* **1970**, *5*, 143. (b) Hathaway, B. J.; Duggan, M.; Murphy, A.; Mullone, J.; Power, C. P.; Walsh, A.; Walsh, B. *Coord. Chem. Rev.* **1981**, *36*, 267. (c) Hathaway, B. J. *Coord. Chem. Rev.* **1983**, *52*, 87. (d) Hathaway, B. J. In *Comprehensive Coordination Chemistry*; Wilkinson, Gillard, and McCleverty, Eds.; Pergamon Press: Oxford, 1985; Vol. 5, p 601.
(19) Solans, X.; Font-Altaba, M.; Oliva, J.; Herrera, J. *Acta Crystallogr.* **1983**, *C39*, 435.
(20) Sundara Rao, R. V. G.; Sundaramma, K.; Sivasankara Rao, G. *Z. Kristallogr.* **1958**, *110*, 231.
(21) Baker, G. A.; Rushbrooke, G. S.; Gilbert, H. E. *Phys. Rev.* **1964**, *135*, A1272.

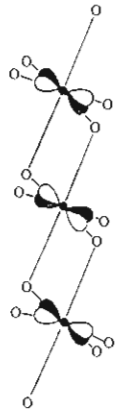

Figure 5. Relative orientation of the copper $d_{x^2-y^2}$ orbitals in the chains.

The best fit (solid lines in Figures 3 and 4) is obtained with the following parameter sets: $g = 2.12$ and $J/k = 0.30$ K for **1**; $g = 2.09$ and $J/k = 0.47$ K for **2**. The magnetic coupling constant, J, can be expressed as a sum of both ferromagnetic (J_F) and antiferromagnetic (J_{AF}) contributions $J = J_F + J_{AF}$.[22] Whereas ferromagnetic contributions are usually small, the magnitude of the antiferromagnetic ones is proportional to the square of the overlap integral between magnetic orbitals,[23] $J_{AF} \propto S^2$.

So, the resulting sign of the magnetic interactions will depend to a great extent on the amplitude of that overlap. Magnetic orbitals are built up from the spin-carrying orbitals of the metals and the symmetry adapted linear combinations of the orbitals of the bridging groups. Given that the idealized local symmetry of the copper atoms is S_4, the ground state of Cu(II) is adequately described by the $d_{x^2-y^2}$ orbital. In the light of the structural features of **1** and **2**, it is evident that these copper orbitals are mismatched to interact between them via formate orbitals (Figure 5). Departures from the idealized symmetry might allow some mixture with the d_{z^2} orbital but, in any case, the overlap would be very poor (Cu–O1–Cu 107.15° (**1**), Cu–O11–Cu 106.46° (**2**)) and $J_{AF} \cong 0$. Thus, the weak ferromagnetic coupling observed for both formate complexes can be reasonably explained in terms of the topology of the bridges between copper atoms.

EPR Spectroscopy. The polycrystalline powder EPR spectra of compounds **1** and **2** are typical of axial environments for copper atoms and lead to $g_\parallel = 2.386$ and $g_\perp = 2.070$, in the case of **1**, and $g_\parallel = 2.384$ and $g_\perp = 2.074$ in the case of **2**. These values fully agree with those expected for elongated $[CuO_6]$ octahedra.[18b]

The single-crystal spectra of **1** were recorded with rotation along three mutually orthogonal directions, X, Y, and Z, where X was parallel to the (011) direction, Y made an angle of 52.7° with the (010) direction, and Z was 7.6° with the (100) direction ($Z = b \times c$). Since there are two magnetically equivalent copper sites in the unit cell, only one signal is observed regardless of the orientation of the external magnetic field. The only copper chain in the unit cell runs parallel to c. Accordingly, at some rotation angle along Z, the directions of the magnetic field and the chain must be coincident.

In the rotation axes frame for the single-crystal experiments on **2**, X and Y were taken parallel to the (010) and (001) directions, respectively, whereas Z made an angle of 11° with the (100) direction. As above, the equivalence of the copper sites in the unit cell leads to only one signal at each angular setting in the external magnetic field. All copper chains are also magnetically equivalent and run parallel to the c axis. So, in the rotation along X and Z the magnetic field moves from being parallel to being perpendicular to the chain direction. The analysis of the angular dependence of the g factors (Figures S3 and S4 in supplementary material) leads to tensor principal component values of $g_1 = 2.391$ and $g_2 = g_3 = 2.070$ for **1** and $g_1 = 2.386$ and $g_2 = g_3 = 2.067$ for **2**, which are in good agreement with the powder data. The orientation matrices of the g values with respect to the orthogonal frame X, Y, and Z are reported in Table IV. Taking the perpendicular to the mean plane corresponding to the equatorial oxygen atoms as one (z) of the preferred directions for the orientation of the g tensor, and locating the other two (x, y) in the intersections of that mean plane with those bisecting the oxygen–copper–oxygen angles, the resulting orientation matrices (Table IV) are, within the experimental error, identical with those experimentally obtained. Hence we can state that the g components follow the symmetry elements of the molecular entities: $g_1 = g_z$; g_2, $g_3 = g_x$, g_y.

Table IV. Experimental Orientation Matrices of the Principal Values of g-Tensors for **1** and **2** Compared to Those for the Molecular x, y, z Directions in the X, Y, Z Framework

	1			2		
g_1	61°	51°	53°	59°	31°	92°
g_2	32°	120°	99°	33°	121°	100°
g_3	102°	126°	38°	80°	93°	10°
g_z	62°	46°	58°	59°	31°	90°
g_x	30°	114°	107°	34°	120°	90°
g_y	91°	127°	37°	90°	90°	1°

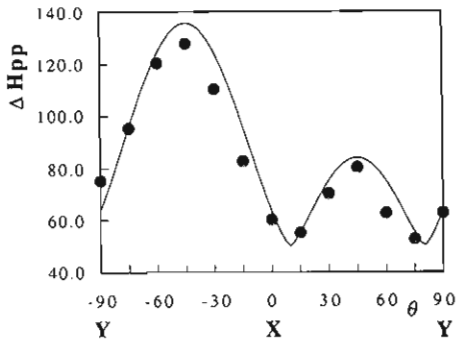

Figure 6. Angular dependence of the line width in $CaCu(HCOO)_4$ at room temperature and 35.5 GHz observed rotating along the Z axis (see text). The solid line represents the calculated values with an escaled $|(3\cos^2\theta) - 1|^{4/3}$ equation.

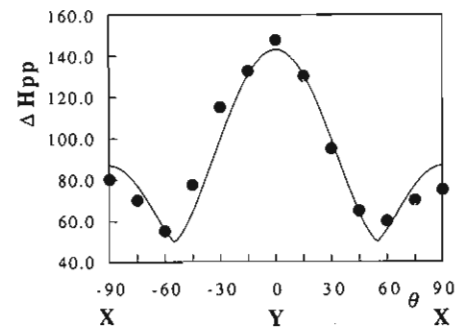

Figure 7. Angular dependence of the line width in $Ca_2Cu(HCOO)_6$ at room temperature and 35.5 GHz observed rotating along the Z axis (see text). The solid line represents the calculated values with an escaled $|(3\cos^2\theta) - 1|^{4/3}$ equation.

Figures 6 and 7 show the angular dependence of the EPR line width when single crystals of **1** and **2**, respectively, were rotated around Z. For **1**, the line width has a maximum (130 G) when the applied magnetic field makes an angle of ca. 45° with the X axis, i.e. when the magnetic field is, within experimental error, parallel to the c axis. Then, it goes through a minimum (60 G) about 55° from the maximum. This magic angle behavior fits nicely to that expected for a one-dimensional ferromagnet. In **2**, the line width again follows a magic angle behavior with the broadest signal observed parallel to the chain direction, this indicating the one-dimensional nature of the compound.[24,25]

(22) Girerd, J. J.; Journaux, Y.; Kahn, O. *Mol. Phys.* **1977**, *34*, 1063.
(23) Kahn, O. *Angew. Chem., Int. Ed. Engl.* **1985**, *24*, 834.
(24) Bencini, A.; Gatteschi, D. *Electron Paramagnetic Resonance of Exchange Coupled Systems*; Springer-Verlag: Berlin, 1990; Chapter 10.
(25) Mcgregor, K. T.; Zoos, Z. G. *J. Chem. Phys.* **1976**, *64*, 2506.

Table V. Magnetic and Structural Parameters[a] for **1** and **2**

	R, Å	Φ, deg	θ, deg	J/k, K
1	2.525	107.15	162.68	0.30
2	2.525	106.46	164.68	0.47

[a] R is the longest Cu–X distance, Φ is the Cu–X–Cu bridging angle, and θ is the X_{eq}–Cu–L_t angle (X_{eq}, equatorial bridging atoms; L_t, oxygen trans to X).

In both compounds the intrachain Cu–Cu separation is about 3.6 Å, whereas the next closest Cu–Cu distances are considerably longer (7.3 Å (**1**), 11.4 Å (**2**)). Since the dipole–dipole contribution to the EPR line widths varies as r^{-6}, the intrachain interactions are the dominant ones in the EPR line widths which must behave as $|(3\cos^2\theta) - 1|^{4/3}$, where θ is the angle between the magnetic field and the chain direction.[24] Shown in Figures 6 and 7 are, besides the experimental EPR line widths, solid lines which follow scaled $|(3\cos^2\theta) - 1|^{4/3}$ equations. The agreement of these functions with the experimental values is a signature of the pure one-dimensional nature of both compounds.

Concluding Remarks

The results presented so far fit into a more general study currently in progress dealing with ordered bimetallic simple carboxylates able to yield cuprates after soft treatments. Prior to this work the only M^{II}–Cu^{II} mixed formates whose structure was known were $CuBa_2(HCOO)_6{\cdot}4H_2O$[20] and $CuSr_2(HCOO)_6{\cdot}8H_2O$.[14] Whereas the high connectivity between copper atoms—via formate bridges—occurring in the different modifications of copper(II) formate, $Cu(HCOO)_2{\cdot}nH_2O$ ($n = 0, 2, 4$),[6,26] is lost in these barium and strontium salts, it seems that it is the lack of water molecules in the calcium salts reported in this work which leads to the above described copper chains. In fact, as pointed out by Hatfield, the topology of these copper chains is common among the bis(μ-ligand)-bridged compounds,[27] but no case was known to date in which both bridging atoms were oxygen ones (apart from the above considerations about a polytype of anhydrous copper(II) formate). Cu_2X_2 moieties usually include halogen atoms and, dealing with carboxylate-containing derivatives, examples of chain compounds involving even only one carboxylate bridge are very scarce.[4,26,28]

The abundance of (μ-halogen)-bridged copper structures allowed the attainment of magneto–structural correlations in these derivatives. It is interesting to note here that the values of J calculated for the title compounds follow the same trends observed with regard to the relevant structural parameters. Listed in Table V are the values of these parameters for **1** and **2**. A detailed discussion of these correlations based on topological and orbital considerations can be found in refs 29 and 30. In the present case, both the departure from planarity of the equatorial donor atoms (measured by θ) and the bridging angle (φ) in **2** work to yield a poorer overlap between the magnetic orbitals, and, consequently, a lesser antiferromagnetic component of the exchange coupling constant. This may explain the observed higher ferromagnetic coupling of **2** with regard to **1**.

Otherwise, in the temperature range investigated, we have not needed to take into account interchain interactions, this meaning that they must be (in absolute value) 1 order of magnitude, at least, smaller than the intrachain ones in both cases. Notwithstanding, given that the Cu–Cu interchain distances vary from 7.295 (2) Å in **1** to 11.326 (2) Å in **2**, it is to be expected that the interchain interactions be, in turn, approximately 1 order of magnitude (in absolute value) smaller in the case of **2**. On this point, further experimental specific heat and susceptibility measurements in the low-temperature range ($T < 4.2$ K) are required in order to confirm the foreseeable maintenance of the one-dimensional character of $Ca_2Cu(HCOO)_6$.

Acknowledgment. This work was supported by the Spanish Comisiõn Interministerial de Ciencia y Tecnología (C.I.C.Y.T. MAT 89-0427 and MAT 90-1020), MIDAS Project (Red Eléctrica de España-UNESA, 89/2017 and 89/3799) and CE89-0010-C02-02 Project. M.J.S. thanks the Spanish Ministerio de Educación y Ciencia for a FPI fellowship. We thank Professor Dirk Reinen (Marburg, Germany) for making available the E15 Varian Spectrometer. We thank Professor J. Alamo (UICM, Universitat de Valencia, Spain) for making available the program to draw Figure S5.

Supplementary Material Available: Table S1 listing crystallographic data and experimental parameters for **1** and **2**, Tables S2–S5 listing atomic coordinates, thermal parameters, bond distances, and angles for **1** and **2**, Tables S7 listing least-squares planes for **1** and **2**, Figure S1 and S2 showing schematic views of the contents of the unit cells of **1** and **2**, Figures S3 and S4 showing the angular dependence of the g-values of **1** and **2** single crystals, and Figure S5 showing the stacking of elongated CuO_4O_2 units in the chains for both compounds (12 pages); Tables S7 and S8 listing the observed and calculated structure factors for **1** and **2** (8 pages). Ordering information is given on any current masthead page.

(26) Towle, D. K.; Hoffmann, S. K.; Hatfield, W. E.; Singh, P.; Chaudhuri, P. *Inorg. Chem.* **1988**, *27*, 394.
(27) Hatfield, W. E. In *Magneto-Structural Correlations in Exchange Coupled Systems*; Willett, R. D., Gatteschi, D., Kahn, O., Eds.; NATO-ASI Series; D. Reidel Publishing Co.: Dordrecht, 1985.
(28) Fuertes, A.; Miravitlles, C.; Escrivá, E.; Coronado, E.; Beltrán, D. *J. Chem. Soc., Dalton Trans.* **1986**, 1795.
(29) Folgado, J. V.; Coronado, E.; Beltrán-Porter, D.; Burriel, R.; Fuertes, A.; Miratvilles, C. *J. Chem. Soc., Dalton Trans.* **1988**, 3041.
(30) Folgado, J. V.; Gómez-Romero, P.; Sapiña, F.; Beltrán-Porter, D. *J. Chem. Soc., Dalton Trans.* **1990**, 2325.